Article:
Liu, M., Konstantinova, M., Negahdar, L. et al. (2021) The role of Zn in the sustainable one-pot synthesis of dimethyl carbonate from carbon dioxide, methanol and propylene oxide. Chemical Engineering Science, 231. 116267. ISSN: 0009-2509

https://doi.org/10.1016/j.ces.2020.116267

Chemical Engineering Science xxx (xxxx) xxx

Contents lists available at ScienceDirect

Chemical Engineering Science

journal homepage: www.elsevier.com/locate/ces

The role of Zn in the sustainable one-pot synthesis of dimethyl carbonate from carbon dioxide, methanol and propylene oxide

Ming Liu [a], Mariia Konstantinova [a], Leila Negahdar [b,c], James McGregor [a,c,*]

[a] University of Sheffield, Department of Chemical and Biological Engineering, Mappin Street, Sheffield S1 3JD, UK
[b] University College London, Department of Chemistry, Gordon Street, London WC1H 0AJ, UK
[c] UK Catalysis Hub, Research Complex at Harwell, Rutherford Appleton Laboratory, Harwell OX11 0FA, UK

HIGHLIGHTS

- Dimethyl carbonate has been successfully synthesised from CO_2, CH_3OH and CH_3CHCH_2O.
- Addition of zinc to the reaction dramatically improves DMC selectivity from 19.8% to 40.2%
- The main influence of zinc is on the transesterification step of the reaction.
- High selectivities to DMC can be achieved at mile reaction conditions.

GRAPHICAL ABSTRACT

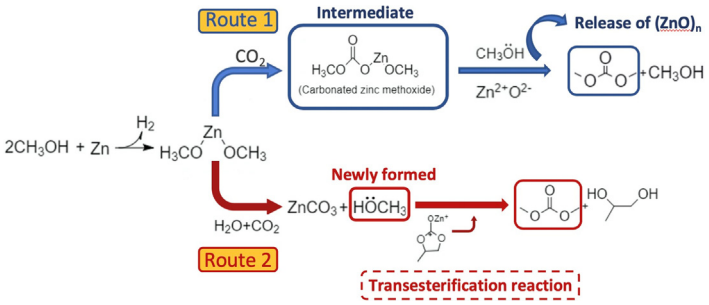

ARTICLE INFO

Article history:
Received 27 May 2020
Received in revised form 20 October 2020
Accepted 31 October 2020
Available online xxxx

Keywords:
Dimethyl carbonate
CO_2
Propylene oxide
Alkali halide catalysts
Zn powder

ABSTRACT

Dimethyl carbonate (DMC) can be applied as a greener alternative to more hazardous materials, *e.g.* phosgene or dimethyl sulfate. Herein, one-pot synthesis of DMC from propylene oxide, methanol and CO_2 using alkali halide catalysts under mild conditions was studied. Addition of Zn powder to the K_2CO_3-NaBr-ZnO catalyst system was seen to increase DMC selectivity from 19.8% (TOF = 39.0 h^{-1}) to 40.2% (TOF = 78.1 h^{-1}) at 20 bar and 160 °C for 5 h. Catalyst characterisation showed that Zn powder increases the stability of the catalyst, preventing the active ingredients on the catalyst surface from leaching. An increase in propylene oxide conversion to DMC is attributed to the increase of Zn^{2+} ions in the reaction solution. Elevated pressure was not found to be a necessary reaction condition for transesterification. This study shows that increased selectivity to DMC can be achieved at mild conditions with the addition of Zn powder.

1. Introduction

Carbon dioxide (CO_2) is most commonly discussed in negative terms as a greenhouse gas and major contributor to anthropogenic climate change. Recently, the use of CO_2 as an abundant carbon resource has received increased attention, with this field referred to as carbon dioxide utilisation. Direct conversion of CO_2 to green chemicals is an attractive application, as it incorporates a waste resource in the production of value-added, sustainable substances. Carbon dioxide utilisation in the synthesis of dimethyl carbonate (DMC) is attractive due to the extensive application of DMC in a variety of processes (Table 1). In particular, DMC has lower toxicity and is a more environmentally friendly chemical compared to traditional alternatives, many of which have unfavourable properties such as high toxicity, *e.g.* phosgene. Based on current global demand, the production of DMC is projected to reach approximately 314 kt by 2025 (Dimethyl Carbonate Market by Application (Polycarbonate, Solvent, Pharmaceutical,

* Corresponding author at: University of Sheffield, Department of Chemical and Biological Engineering, Mappin Street, Sheffield S1 3JD, UK.
E-mail address: james.mcgregor@sheffield.ac.uk (J. McGregor).

https://doi.org/10.1016/j.ces.2020.116267
0009-2509/

Table 1
Application of dimethyl carbonate as a green chemical.

Application	Chemicals replaced by DMC	Advantage of using DMC	Reference
Methoxycarbonylating agent	Phosgene ($COCl_2$)	Selective reaction towards non-toxic products. Less hazardous reagent	(Aricò and Tundo, 2010)
Methylating agent	Dimethyl sulfate (DMS) or methyl halide (CH_3X, X = I, Br, Cl)	Higher selectivity to mono-methylated derivatives and less harmful to environment.	(Selva et al., 1994)
Gasoline additive	Methyl *tert*-butyl ether (MTBE)	Increases octane number which reduces the total emissions of hydrocarbons, carbon monoxide and formaldehyde.	(Pacheco and Marshall, 1997)

Pesticide) - Growth, Share, Opportnities & Competitive Analysis, 2017–2025, 2017).

Conventional methods of DMC synthesis require the use of hazardous gases such as carbon monoxide (CO) or phosgene ($COCl_2$). Alternatively, the direct synthesis of DMC from methanol (CH_3OH) and CO_2 is a promising alternative due to high atom efficiency, low toxicity, and the use of readily-available feedstocks (Sakakura and Kohno, 2009). However, this process is limited by low conversion due to its endothermic and endergonic nature (ΔG = +26 kJ/mol) (Eta and Leino, 2010). Thermodynamic limitations can be overcome by employing a two-step conversion from epoxide compounds such as ethylene oxide or propylene oxide, thereby increasing the yield of DMC. Two-step conversion results in the formation of a cyclic carbonate intermediate, which can be synthesised using single component catalysts (*e.g.* polymeric organocatalyst) (Subramanian et al., 2018) or simple hybrid systems (*e.g.* Cesium salts) (Suleman et al., 2019), however, the intermediate must be separated in a cost-intensive process such as filtration of the catalyst and evaporation of residual PO. Therefore, high conversion *via* a one-pot synthesis of DMC is highly desirable. Herein we report the one pot synthesis of DMC using CO_2, methanol and propylene oxide in the presence of metal alkali halide catalysts.

The one-pot synthesis of DMC consists of two reversible steps: cycloaddition and transesterification. In the cycloaddition reaction, propylene oxide reacts with CO_2 to form propylene carbonate (PC) (Scheme 1). In the transesterification step, methanol and PC are converted to DMC and propylene glycol (PG). 1-methoxy-2-propanol and 2-methoxy-1-propanol are produced as by-products through the reaction between PO and methanol. The overall selectivity to DMC is limited by the formation of PG as a by-product *via* hydrolysis of PO by water formed in the reaction. Selectivity to DMC can therefore be increased by reducing the rate of production of PG through removing water from the system by adding dehydrating agents. Solid dehydrating agents can be used to remove water from the process, but most such agents *e.g.* 3 Å molecular sieve, are not effective at high temperatures or pressures. 3 Å molecular sieve is effective for dehydration only under 100 °C as the adsorption capacity decreases with increasing temperature (Simo et al., 2009). Therefore, it is necessary to find alternative agents for removing water from the system.

Another desirable process consideration is the ability to operate under relatively mild conditions. Previously, high selectivity to DMC has been correlated with high pressure operating environments employing supercritical CO_2. Table 2 summarises the selectivity to DMC achieved over various catalysts at different CO_2 pressures. TOF values of the catalytic systems are calculated based on the reaction conditions provided in the previous literature studies. Applying high-operating pressure in chemical plants is, however, cost and energy intensive and introduces significant safety concerns. Optimisation of reaction conditions with the aim of minimizing the operating pressure while increasing reaction rate, selectivity and catalyst lifetime should be a key goal of process development (The Royal Society, 2017).

The choice of catalyst is also a crucial parameter in achieving high yields of DMC. It is known that alkali halides activate the cycloaddition reaction (Scheme 1) by nucleophilic attack of halide ions in the first step of reaction (Martínez-Ferraté et al., 2018). For example, KI immobilised on ZnO is an effective catalyst under supercritical conditions (Chang et al., 2004). The addition of a strong base such as KOH, K_2CO_3, KNO_3 or Na_2CO_3, to the catalyst can improve selectivity to DMC by increasing the availability of basic sites, thereby promoting transesterification (Wang et al., 2016). Additionally, promotors may be added to improve the yield of DMC. For example, Mg turnings have been employed as a co-catalyst alongside KCl-promoted ZrO_2. Mg produces $Mg(OCH_3)_2$ as an intermediate product which can react with carbon dioxide to form carbonated magnesium methoxide (CMM) (Eta et al., 2010). The exchange of oxygen atoms between methoxy groups of CMM adsorbed on catalyst surface and the bulk oxygen of catalyst enhances the production of DMC. MgO has also been employed by De and co-workers in combination with a supported basic ionic liquid-choline hydroxide (De et al., 2009). A review of the role of

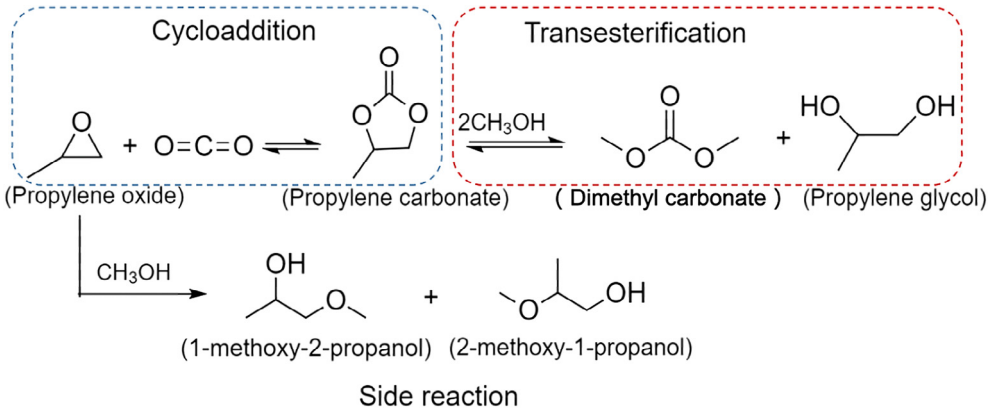

Scheme 1. Reaction pathway of one-pot synthesis of DMC.

Table 2
Catalysts previously applied in the one-pot synthesis of DMC, and CO_2 pressures employed.

Catalyst	CO_2 pressure (bar)	DMC selectivity	TOF (h^{-1})	Reference
KOH-KI-ZnO	165	58.0%	8.4	(Chang et al. 2004)
Mg-KCl-ZrO_2	95	52.7%	52.2	(Eta et al., 2010)
MgO	80	13.6%	4.1	(Bhanage et al., 2001)
KOH-4A	30	16.8%	41.9	(Li et al., 2005)
Na_2CO_3–KCl-Al_2O_3	25	20.1%	–	(Jiang and Yang, 2004)
KCl + crown ethers	20	23.0%	73.7	(Li et al., 2015)
KOH-β-zeolite	20	23.3%	–	(Xu et al., 2013)

alkali metal salts in catalytic carbon dioxide utilisation is provided by Truong and Mishra (Truong and Mishra, 2020).

This work therefore considers the application of ZnO-supported NaBr (as an alkali halide) promoted with K_2CO_3 (as a strong base) in the synthesis of DMC from CO_2, methanol and PO at 160 °C and 20 bar over a reaction time of 5 h. Based on previous literature research (Liu et al., 2016), the introduction of nucleophilic group such as Cl^-, Br^- or I^- facilitates the coupling the reaction of propylene oxide and CO_2. The catalytic activity decreases in the order of $I^- > Br^- > Cl^-$, which is in agreement with the ability of nucleophiles to donate electrons and the leaving ability of the halide anions. Therefore, the proposed ZnO carrier with the nucleophilic Br^- anion is applied in this research: iodide compounds are less cost effective and present toxicity concerns. Alkali metal carbonate (K_2CO_3) is used to increase the intensity of strong basic sites on the catalyst surface due to the formation of potassium oxide during the calcination procedure (Jiang and Yang, 2004). Supported K_2CO_3 catalysts have also been investigated by Tian and co-workers (Tian et al., 2007); the synthesised catalysts exhibited excellent catalyst recyclability. Since zinc powder can react with water vapour to form zinc oxide, zinc can potentially act as a dehydrating agent and increase the selectivity to DMC by reducing the formation of PG. The role of metallic zinc and the possible reaction mechanism are presented and discussed. As magnesium methoxide (formed by the reaction of MgO and methanol) has previously been reported as a reaction intermediate in the presence of Mg, the formation of zinc methoxide as an intermediate in the presence of Zn was therefore expected. In this study, magnesium methoxide was also used to investigate the possible reaction mechanism in order to deconvolve the influence of the metal powder from the metal oxide support. Furthermore, the surface properties of the catalyst system were analysed and reported.

2. Experimental

2.1. Materials

Reagents sodium bromide (≥99%), potassium carbonate (≥99%), methanol (≥99.9%) and propylene oxide (≥99.5%) were purchased from Sigma-Aldrich. Zinc oxide (≥99%) was purchased from Fisher Scientific. Carbon dioxide gas (≥99.99%, water content < 0.01%) was obtained from BOC. 2-propanol (Sigma-Aldrich, ≥99.8%) was used as an internal standard for GC–FID quantitative analysis. Dimethyl carbonate (99%), propylene carbonate (99.7%), 1-methoxy-2-propanol (≥99.5%) and propylene glycol (≥99.5%), supplied from Sigma Aldrich, were employed as reference materials for calibration curves. All materials were used as received unless otherwise stated.

2.2. Catalyst preparation

Prior to impregnation, the metal oxide support (ZnO) was calcined at 700 °C for 3 h. K_2CO_3-NaBr-ZnO was synthesised by addition of 12 wt% K_2CO_3 and 17.5 wt% NaBr to ZnO by wet impregnation. The mixture was refluxed at 60 °C for 24 h, followed by vacuum filtration. Based on a method previously reported by Chang et al. (2004), filtered solids were dried at 100 °C for 12 h and then further calcined at 700 °C for 3 h. The catalyst composition was selected on the basis of preliminary screening studies employing varying K_2CO_3 and NaBr contents. The selected composition gave the highest DMC selectivity with relatively low selectivity to PG and by-products as shown in Figure S1. Preliminary studies (Figure S2) also confirmed that improved performance was obtained when using bromide salts rather than chloride salts in agreement with the known trends in their nucleophilicity (Section 1); additionally, the use of Na_2CO_3 as the carbonate was observed to result in lower yields of DMC than when using K_2CO_3 (Figure S3).

2.3. Catalytic synthesis of DMC

The one-pot synthesis of dimethyl carbonate was carried out in a stainless-steel reactor (Parr Instruments, Model 4714) equipped with an external thermometer and a heating jacket. The reactor was placed on an electric heater equipped with a mechanical stirrer. In a typical reaction, 100 mmol methanol, 33.3 mmol propylene oxide and 0.3 g catalyst were loaded into the reactor. A molar ratio of 1 to 5 Zn:PO was used with a PO concentration of 33.3 mmol. Air in the autoclave was removed by purging three times with CO_2. The reactor was then pressurised with CO_2 to 20 bar at room temperature before heating to 160 °C. The stirrer was then turned on, indicating time zero, and the reaction run for 5 h. The pressure of the reactor was measured by a pressure gauge equipped with pressure relief valve. At the end of the desired reaction time, the reactor was quenched in an ice-water bath and cooled to 10 °C. Acetone and 2-propanol were used as the solvent and internal standard for GC-FID measurements (Section 2.4). In experiments where $Mg(OCH_3)_2$ was employed, this was added in the liquid-phase alongside the other reactants prior to reaction

Qualitative analysis of reaction liquid samples was performed by GC–MS (Shimadzu GCMS QP2012SE). The temperature of the GC column was held at 40 °C for 2 min and was programmed to rise to 180 °C at a rate of 10 °C min^{-1}, then to further increase to 230 °C at a rate of 10 °C min^{-1} and held at that temperature for 3 min. GC-FID was employed for quantitative analysis based on experimental calibration curves with 2–propanol being used as the internal standard. The yield and selectivity of products and PO conversion were calculated based on the amount of each product and the amount of PO added (Li et al., 2015). Turnover frequency (TOF) is used to evaluate the catalytic efficiency of the reaction system. This is typically defined as the number of molecules reacting per active site per unit time [21]. It is however challenging to determine the quantity of active sites in a heterogeneous catalyst with a non-uniform surface. Therefore, in this work, TOF is defined as the mass of synthesised dimethyl carbonate (DMC) per gram of catalyst per hour [21] as shown in Equation 1:

$$\mathrm{TOF} = \frac{m_{DMC}}{W_{cat} \times t} = \frac{n_{PO} \times Yield_{DMC} \times M_{DMC}}{W_{cat} \times t}$$

where n_{PO}, M_{DMC}, t, and W_{cat}. represent the molar amount (mmol) of PO, formula weight (g mol^{-1}) of DMC, reaction time (h) of DMC synthesis reaction, and the mass of overall catalyst (mg), respectively. Multiple measurements were used for each TOF calculation and the average of those is presented.

2.4. Catalyst characterisation

The catalysts were characterised through BET adsorption isotherms and BJH pore volume analysis, thermogravimetric analysis (TGA), X-ray diffraction (XRD), scanning electron microscopy-energy dispersive X-ray (SEM-EDX) spectroscopy, inductively coupled plasma mass spectrometry (ICP-MS) and atomic absorption spectroscopy (AAS).

The specific surface area (BET) and pore size distribution (BJH) of K_2CO_3-NaBr-ZnO was measured with a Quadrasorb EVO instrument (model QDS-30), using the adsorption of N_2 at the temperature of liquid nitrogen (77 K). Prior to measuring, the sample was degassed at 523 K for 24 h and finally outgassed to 10^{-3} Torr.

Thermogravimetric analysis of catalysts was performed on a thermogravimetric analyser (PerkinElmer, TGA 4000) employing ~ 6 mg of sample and increasing temperature to 950 °C at 10 °C min^{-1} under a stream of N_2 (20 ml min^{-1}).

X-ray diffraction was employed to analyse the morphological properties of the catalyst. Samples were analysed using a Bruker D2 Phaser powder XRD instrument with Cu Kα (30 kV, 10 mA) radiation at a scanning rate of 0.05° min^{-1}. Scanning electron micrographs and EDX were recorded on a JSM-6010LA JEOL SEM instrument with AGAR Sputter Coater. All the samples were coated with a gold layer and analysed at 10 keV with a working distance of 10 mm.

Atomic absorption spectroscopy (AAS) and inductively coupled plasma-optical emission spectrometry (ICP-OES) were employed to analyse the spent solid catalyst and liquid reaction products. In a typical sample preparation procedure, both solid and liquid sample were digested with concentrated HNO_3, followed by dilution of digested solutions with 1% HNO_3 solution (concentration < 10 ppm).

3. Results and discussion

3.1. Catalytic activity of K_2CO_3-NaBr-ZnO, Zn powder and magnesium methoxide

The catalytic activity towards DMC synthesis displayed by the unpromoted catalyst (NaBr-ZnO), and base-promoted catalyst (K_2CO_3-NaBr-ZnO) with and without zinc powder and magnesium methoxide are summarised in Table 3, alongside data for Zn powder and $Mg(OCH_3)_2$ alone.

As anticipated, the addition of the base, K_2CO_3, increases the selectivity to DMC – specifically from 13.8% to 19.8% and decreases selectivity to PC (Table 3, entries I and II). This suggests that K_2CO_3 promotes the transesterification of PC and methanol to DMC. This is consistent with previous observations on the role of basic promoters (Section 1). The addition of Zn powder to the reaction results in an even more dramatic increase in DMC yield from 19.8% to 40.2% with a TOF of 39.0 h^{-1} and 78.1 h^{-1}, respectively. This is comparable to results achieved in supercritical CO_2 (Table 2, highest TOF = 73.7 h^{-1} with KCl + crown ether catalyst) despite the reaction herein being conducted at relatively mild conditions. However, selectivity to PG (35.9%) is similar to that of DMC (40.2%) in this system because PG is generated simultaneously with DMC with a molar ratio of 1 to 1 during the transesterification reaction. It is also evident that more by-products are formed with the addition of zinc (Table 3), which is a key factor inhibiting DMC formation. Increased formation of 1-methoxy-2-propanol and 2-methoxy-1-propanol is observed from the reaction of methanol with PO (Scheme 2). Note that Zn powder on its own has only limited activity (entry IV), with 54.5% PO conversion as compared to > 98% in all other cases, and negligible (0.3%) selectivity to DMC.

The impact of Zn on the reaction is proposed to result in two effects. Firstly, as a dehydrating agent Zn removes water from the reaction. Secondly, Zn forms zinc methoxide ($Zn(OCH_3)_2$) *via* reaction with methanol. Metal methoxides are well-known homogeneous transesterification catalysts, *e.g.* sodium or potassium methoxide is typically generated *in situ* during biodiesel synthesis from oils or fats (Balat, 2007). Therefore, it is expected that Zn promotes the second stage of the reaction, transesterification. However, it is challenging to decouple the effects of Zn added as zinc powder and Zn present in the ZnO support. Therefore, in order to investigate the catalytic activity of metal methoxides, the effect of adding $Mg(OCH_3)_2$ was investigated. $Mg(OCH_3)_2$ contains the same methoxy group as $Zn(OCH_3)_2$, but solid products formed in the reaction, such as MgO, $Mg(OH)_2$ or $MgCO_3$, can be readily distinguished from those formed from the ZnO support. The results show that $Mg(OCH_3)_2$ contributes to the formation of DMC regardless of the presence (selectivity of 43.2%) or absence (selectivity of 34.4%) of the solid catalyst in the reaction. Hence, $Mg(OCH_3)_2$ can successfully catalyse both steps in the one-pot reaction system.

With the addition of either Zn powder or $Mg(OCH_3)_2$, the selectivity to PC in the final liquid product decreases (Table 3, entries II, III, V). This is indicative of higher conversion of PC to DMC. A possible explanation for the increased DMC yield in these systems is an increase in the concentration of methoxy groups from Zn $(OCH_3)_2$ in the liquid phase, which promote transesterification. It can therefore be concluded that Zn powder acts as a promoter rather than only as a dehydrating agent in the reaction.

Table 3
Catalytic activity of DMC catalysts.

Entry	Catalyst	PO conversion (%)	DMC formed (mmol/ml)	Selectivity (%)				TOF (h^{-1})
				DMC	PC	PG	By-product	
I	NaBr-ZnO [a]	98.6	0.97	13.8	66.6	18.1	8.8	27.2
II	K_2CO_3-NaBr-ZnO	98.3	0.84	19.8	36.5	26.1	18.0	39.0
III	K_2CO_3-NaBr-ZnO + Zn	97.0	1.67	40.2	23.4	35.9	39.7	78.1
IV	Zn powder	54.5	0.006	0.3	0.3	6.7	92.2	–
V	K_2CO_3-NaBr-ZnO + $Mg(OCH_3)_2$ [b]	99.1	1.64	43.2	33.7	29.1	30.9	85.7
VI	K_2CO_3-NaBr-ZnO + $Mg(OCH_3)_2$ + Zn	96.4	1.53	37.6	27.1	26.5	36.8	72.5
VII	$Mg(OCH_3)_2$	99.6	1.47	34.4	17.3	22.8	33.9	–

Reaction conditions: 20 bar CO_2, 160° C, 5 h. [a] Methanol (100 mmol), PO (33.33 mmol), catalyst (0.3 g), Zn powder (0.43 g); [b] 3.3 mmol $Mg(OCH_3)_2$ and 100 mmol methanol, PO (33.3 mmol), catalyst (0.3 g), Zn powder (0.43 g); PO: propylene oxide, PC: propylene carbonate, PG: propylene glycol, By-products: 2-methoxy-1-propanol and 1-methoxy-2-propanol. The standard deviation is within ± 3.5% of the reported selectivity.

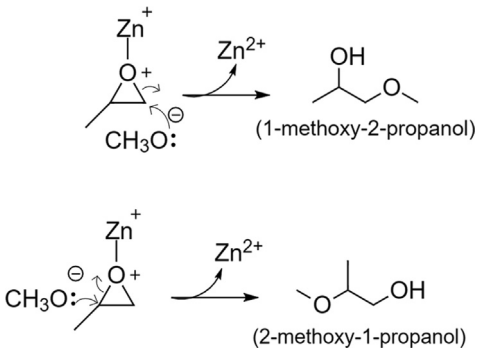

Scheme 2. Proposed reaction mechanism for the formation of by-products in the synthesis of DMC from propylene oxide, CO_2 and methanol.

3.2. The role of Zn powder

As shown in Table 3, the addition of zinc has a notable effect on the reaction, for example, adding zinc powder alongside K_2CO_3-NaBr-ZnO increases selectivity to DMC from 13.8% to 40.2%. As discussed in Section 1, the synthesis of DMC is a stepwise reaction involving cycloaddition, followed by transesterification (Scheme 1). In order to determine the role of zinc, its influence in each of these steps was investigated independently. The role of Zn in the cycloaddition reaction is investigated in Section 3.2.1, while its role in transesterification is reported in Section 3.2.2.

3.2.1. The role of zinc in the cycloaddition reaction

The production of propylene carbonate is limited by the hydrolysis of propylene oxide to propylene glycol. In order to investigate the influence of Zn, a systematic comparison of the yields of propylene carbonate and propylene glycol, and propylene oxide conversion in the presence of different reactants and catalysts were conducted. Fig. 1 shows the influence of zinc on the reaction in the presence of: (i) propylene oxide, CO_2 and catalyst only (reactions 1 and 2); (ii) PO, CO_2, catalyst and water (reactions 3 and 4); and (iii) PO, CO_2, catalyst and PG (but no water) (reactions 5 and 6).

In each case, the effect of Zn on the cycloaddition reaction does not appear to be significant. Specifically, when only CO_2, PO and catalyst are involved in the reaction, there is no change in PO conversion and PC yield, while PG yield is approximately halved

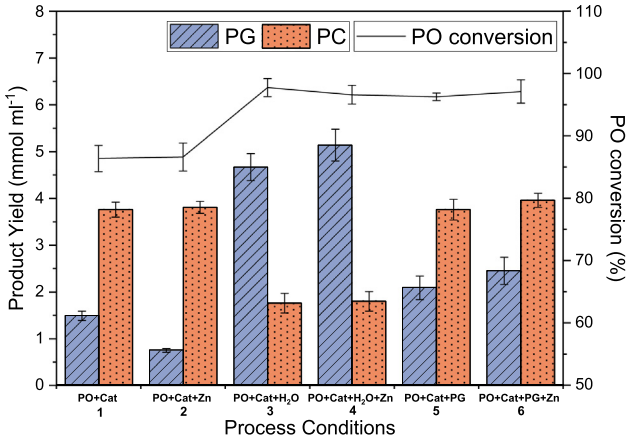

Fig. 1. Conversion of PO and the yields of PG and PC in the one-pot synthesis of DMC. Reaction conditions: 160 °C, 5 h, CO_2 (20 bar); catalyst (K_2CO_3-NaBr/ZnO, 0.3 g), Zn powder (0.43 g), PO (66.7 mmol), H_2O (44.4 mmol, reactions 3 and 4), PG (11.1 mmol, reactions 5 and 6).

to ~ 0.7 mmol/ml. When water or PG is present in the reaction, PG production is increased by 10.1% and 17.2%, respectively, while the PC yield does not change.

The reaction mechanism for the formation of propylene carbonate by halides is well established. Carbon dioxide is a weakly acidic gas which can adsorb or react at acid-base sites on solid surfaces. In previous studies where the mechanism of cycloaddition has been discussed, the reaction is proposed to be initiated by the attack of the Br^- nucleophile on the epoxide followed by reaction of the alkoxide with CO_2 and finally by ring-closure (Wang et al., 2012). At the same time, Zn^{2+} and Br^- dissociate from the product and dissolve into the reaction solution. The Zn surface might contribute to the activation of the epoxide via Zn(II) atoms but also via Zn-OH groups acting as hydrogen bond donors (Lagarde et al., 2019). Following this mechanism, it would be expected that the addition of Zn powder would have little effect on PC formation, in line with the experimental results presented in Fig. 1.

3.2.2. The role of zinc in the transesterification reaction

The effect of both Zn powder and CO_2 on transesterification is explored in this study. To the best knowledge of the authors, the role of carbon dioxide in the second step of DMC synthesis has not previously been discussed in literature. Fig. 2 demonstrates the effect of zinc on the reaction when, (i) PC, methanol and CO_2 are all present (reactions 7 and 8); (ii) PC and methanol are present but in the absence of CO_2 and at atmospheric pressure (reaction 9); and (iii) PC and methanol are present, CO_2 is absent and the reaction mixture is under an initial (room temperature) atmosphere of helium gas at 20 bar (reaction 10). These are compared to the reaction with PG, methanol and CO_2 in the absence of Zn as a baseline case (reaction 7). It is seen that Zn powder has a significant effect on transesterification by simultaneously increasing the conversion of PC and the yield of DMC, with a three-fold increase in the TOF values (from 20.8 h^{-1} to 66.0 h^{-1}). In the absence of Zn powder, the yield of PG (1.15 mmol ml^{-1}) is much higher than that of DMC (0.51 mmol ml^{-1}). In contrast, the ratio of PG and DMC formed in the presence of Zn is approximately equal (1.70 mmol $ml^{-1}$and 1.62 mmol ml^{-1}, respectively).

The presence of Zn^{2+} ions may explain the increase in DMC selectivity observed in the presence of Zn powder (Scheme 3). The reaction starts with the attack of the zinc ion by the carbonyl of PC, then the methoxy groups of methanol attack the carbon atom in intermediate 1. DMC and PG are then formed by the transfer of H^+ (Murugan and Bajaj, 2010). However, the higher PC conversion and higher PG yield obtained may also indicate that there is an alternative reaction route to convert PC to DMC bypassing the formation of PG.

Considering the role of the gas atmosphere, in the absence of CO_2 (reaction 10) and at atmospheric pressure (reaction 9) produced yields of DMC and PG are very similar to those obtained under 20 bar CO_2 (reaction 8). However, in contrast to reaction 9, DMC (1.71 mmol ml^{-1}) is produced in greater quantities than PG (1.57 mmol ml^{-1}). Notably, 0.10 mmol ml^{-1} of PO is formed in the absence of CO_2 at atmospheric pressure. This is not observed under 20 bar CO_2. Under 20 bar He, but not CO_2, the highest TOF of 80.8 h^{-1} is obtained. Moreover, production of DMC increased by 22.8% and that of PG increased by 15.9% as compared to the values obtained under 20 bar CO_2. PO was also observed to form under 20 bar He, at a concentration of ~ 0.13 mmol ml^{-1}, similar to that obtained at ambient pressure in the absence of CO_2.

In the cycloaddition reaction CO_2 is a reactant, and hence propylene carbonate production is enhanced by increasing CO_2partial pressure. The similarity of the yields of DMC and PG obtained under 20 bar CO_2, under 20 bar He and at ambient pressure, however, indicates that elevated pressure is not required for transesterification to proceed. However, CO_2 does influence the reverse

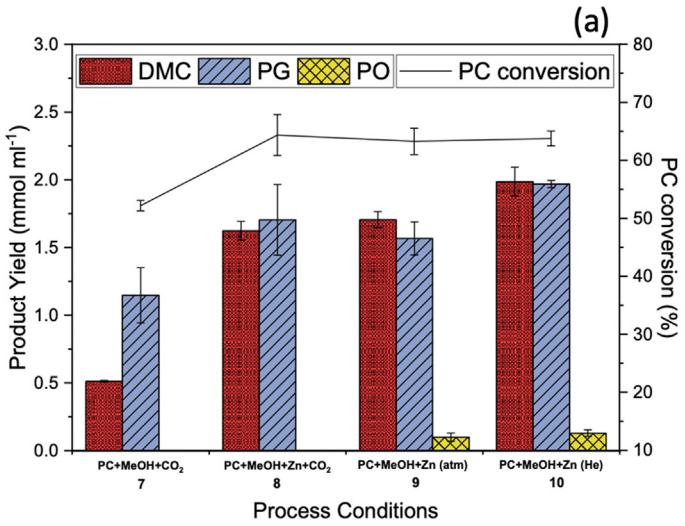

(b)

Reaction No.	TOF (h^{-1})
7	20.8
8	66.0
9	69.3
10	80.8

Fig. 2. (a) Conversion of PC and the yield of DMC, PG and PO in the one-pot synthesis of DMC. (b) The activity of catalyst under various reaction conditions. Reaction conditions: 160 °C, 5 h, CO_2 (20 bar, reactions 7 and 8 only), He (20 bar, reaction 10 only), catalyst (K_2CO_3-NaBr-ZnO, 0.3 g), PC (33.3 mmol) and methanol (100 mmol). Zn powder (0.43 g) is also present in reactions 8–10.

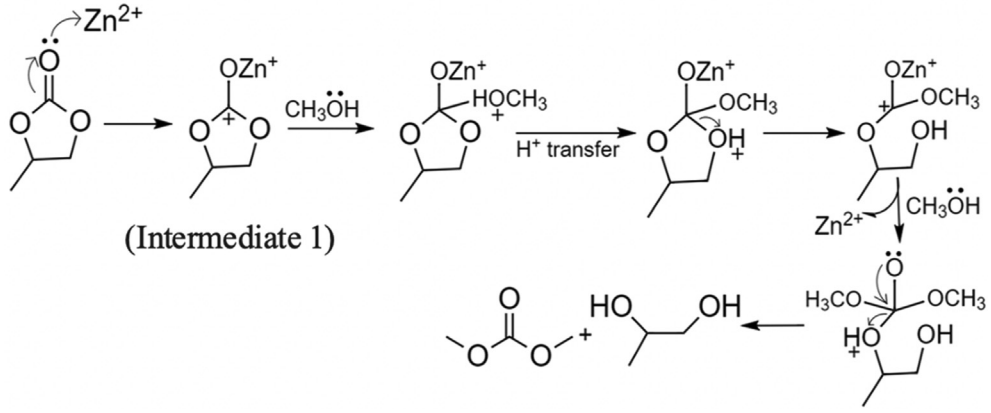

Scheme 3. Proposed mechanism for the synthesis of dimethyl carbonate from propylene carbonate and methanol.

cycloaddition reaction, as evidenced by the presence of PO in reactions at atmospheric pressure and under 20 bar He, but not under CO_2. CO_2 therefore limits the formation of undesired by-products. The suppression of the reverse cycloaddition reaction and decreased DMC yield may indicate poisoning of active sites of the catalyst by CO_2. Previous studies at 5 bar CO_2 have indicted the successful synthesis of DMC from ethylene oxide (Liu et al., 2015).

3.3. Catalyst characterisation

3.3.1. Thermogravimetric analysis

Thermogravimetric analysis was used to investigate the interaction between the active components - K_2CO_3 and NaBr - and the support, and the effects of the calcination step during catalyst synthesis (Chen and Marks, 2000). The thermogravimetric analysis of two samples, (a) uncalcined K_2CO_3–NaBr–ZnO and (b) a mixture of K_2CO_3, NaBr and ZnO, is shown in Fig. 3. The original TGA data are plotted alongside the differential thermograms (DTG).

It can be seen from the TG and DTG plots in Fig. 3(a) that the uncalcined catalyst exhibits a weight loss in the temperature range of 720–830 °C, and reaches a maximum weight loss rate at ~ 800 °C. During the catalyst preparation process, the active species (K_2CO_3 and NaBr) in the solution are attached to the surface of the support. The weight loss is associated with decomposition of carbonate group in the newly formed compound slightly below 800 °C (Fierro et al., 2002). The TG-DTG curve in Fig. 3(b) shows that the weight of the mixture starts to decrease from ~ 750 °C, and the rate of mass loss reaches a maximum at ~ 920 °C due to the decomposition of K_2CO_3 (Sun et al., 2014). Comparing Fig. 3 (a) and 3(b), it can be concluded that a new polymer is formed during the preparation of the catalyst. The calcination temperature of the catalyst was therefore selected as 700 °C because the structure of the catalyst is unstable above 720° C.

3.3.2. X-ray diffraction

XRD was used to study the composition of solid catalyst before and after reaction with $Mg(OCH_3)_2$ in order to deconvolve the role of Zn in the reaction. The XRD pattern of the solid reaction products in the presence of the catalyst and $Mg(OCH_3)_2$, and in the presence of only $Mg(OCH_3)_2$ are presented in Fig. 4. The typical peaks of $MgCO_3$ (PDF-ICDD 04–012-1188) are apparent in the solid products obtained under both reaction conditions. The remaining peaks shown in Fig. 4(a) are assigned to $Mg_{0.1}Zn_{0.9}O$ (PDF-ICDD04-019–9591).

According to the $Mg(OCH_3)_2$-promoted reaction mechanism previously proposed (Eta et al., 2010), $Mg(OCH_3)_2$ and

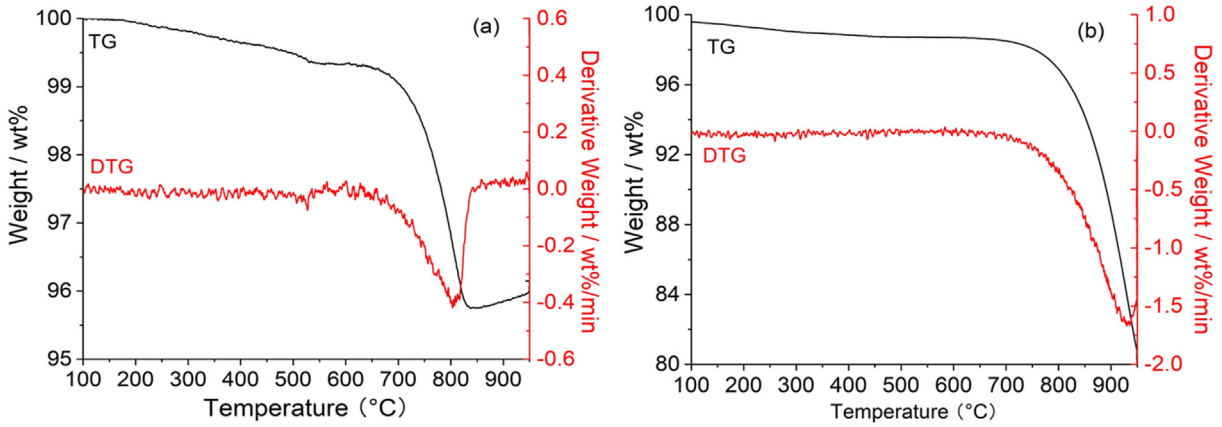

Fig. 3. DTG and TG curves of (a) uncalcined K_2CO_3-NaBr-ZnO (b) mixture of K_2CO_3, NaBr and ZnO.

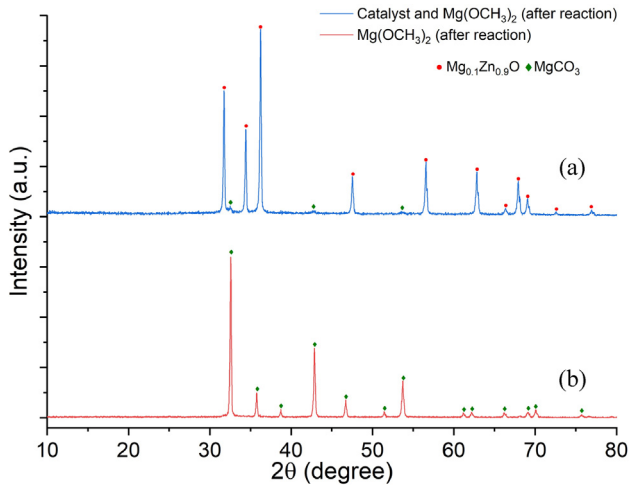

Fig. 4. The XRD patterns of reaction products resulting from: (a) reaction with catalyst and $Mg(OCH_3)_2$; and (b) reaction with $Mg(OCH_3)_2$ only.

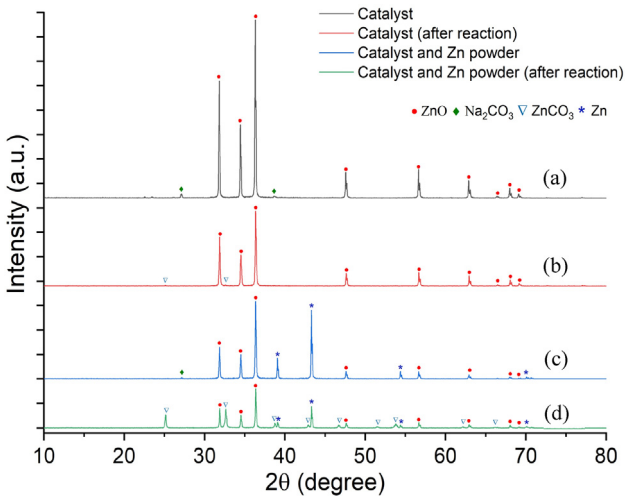

Fig. 5. The XRD patterns of fresh and spent catalysts: (a) fresh K_2CO_3-NaBr-ZnO; (b) K_2CO_3-NaBr-ZnO after reaction; (c) fresh K_2CO_3-NaBr-ZnO and Zn powder mixture; and (d) K_2CO_3-NaBr-ZnO and Zn powder mixture after reaction.

K_2CO_3-NaBr-ZnO participate as shown in Scheme 4. Bidentate carbonate is formed as an intermediate, indicative of the migration of CO_3 species from CMM to the surface of catalyst. The exchange of oxygen atoms between the intermediate and the catalyst ultimately results in the production of DMC. The formation of DMC is completed with the release of $Mg_{0.1}Zn_{0.9}O$.

Diffractograms of the fresh and spent catalyst are shown in Fig. 5. The presence of ZnO (PDF-ICDD 01–081-8838) and Na_2CO_3 (PDF-ICDD 04–013-9890) are clearly present in the fresh catalyst (K_2CO_3-NaBr-ZnO). The diffractogram of the spent catalyst (Fig. 5 (b)) shows the appearance of $ZnCO_3$ (PDF-ICDD 04–015-6717). This

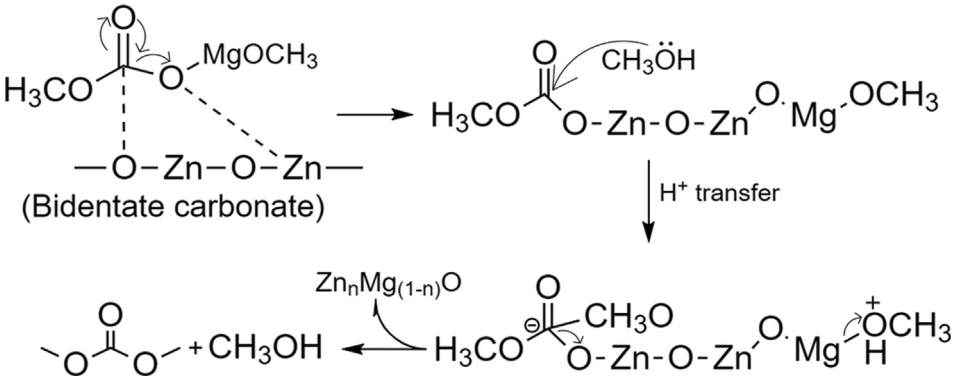

Scheme 4. Proposed mechanism for the reaction with $Mg(OCH_3)_2$ when using K_2CO_3-NaBr-ZnO as catalyst (adapted from the reaction mechanism of $Mg(OCH_3)_2$-promoted reactions, proposed by Eta *et al.* (Eta et al., 2010).

indicates that the stable carbonyl double bond is disrupted as a result of the reaction of CO_2 with the active site of catalyst.

The mixture of K_2CO_3-NaBr-ZnO and Zn powder (Fig. 5(c)) is found to contain Zn (PDF-ICDD 04–014-0235), ZnO (PDF-ICDD 01–083-8004), and Na_2CO_3(PDF-ICDD 04–013-9890). $ZnCO_3$ (PDF-ICDD 04–015-6717) is formed after the reaction, with higher peak intensities *cf.* Fig. 5(b) indicating that the content or crystallinity of $ZnCO_3$ is increased (see Table 4). The full width at half maximum (FWHM) of the peak obtained from the XRD pattern is used to calculate the crystallite size of particles by using the Scherrer equation (Patterson, 1939).

The crystallite size of ZnO remains essentially unchanged before and after the reaction when only the catalyst is involved (Table 4). However, when zinc powder is added, the crystallite size of ZnO increases by approximately 6 nm after reaction, and the average size of Zn powder decreases from 54 nm to 45 nm. This is consistent with the hypothesis that zinc powder converts to ZnO and $ZnCO_3$ during reaction. The reaction with $Mg(OCH_3)_2$ yields analogous solid products ($Mg_{0.1}Zn_{0.9}O$ and $MgCO_3$, Fig. 4) indicating that both Zn and Mg may undergo transformation *via* similar reaction mechanisms. Based on the reaction mechanism of $Mg(OCH_3)_2$ (Scheme 4), it is possible to speculate the reaction mechanism of zinc. The Zn powder is converted to $Zn(OCH_3)_2$ and subsequently reacts with CO_2 to form carbonated zinc methoxide (CZM). The carbonate group of CZM is adsorbed on the surface of the catalyst at unsaturated $Zn^{2+}O^{2-}$ Lewis acid-base pair sites and the intermediate bidentate carbonate is formed. The exchange of oxygen atoms in the bidentate carbonate with the oxygen atoms on the catalyst surface results in migration of the carbonate species on the catalyst surface, which facilitates the formation of DMC.

3.3.3. Textural properties

BET adsorption isotherms yield a surface area of 1.4 m^2g^{-1}, while BJH pore size analysis yields a pore volume of 3.9 cm^3g^{-1} and a pore diameter centred around 3.8 nm. The full pore size distribution is shown in Figure S4.

SEM and EDX analysis provide information regarding the morphology and the elemental composition of the catalyst. Fig. 6 shows the surface morphology of the solid products from reactions involving $Mg(OCH_3)_2$. It is apparent that the shape of the granular catalyst is unchanged before and after the reaction (Fig. 6(c) and 6 (b), respectively). As $Mg(OCH_3)_2$ acts as a homogeneous catalyst in the reaction (Section 3.1), the reaction pathway described by Scheme 4 is proposed as the major route for the formation of DMC. Based on XRD analysis (Fig. 4), agglomerates of $MgCO_3$ are formed during the reaction; an example of this can be seen in Fig. 6(a).

SEM analysis of the mixtures of the catalyst with zinc powder are shown in Fig. 7. Granular morphology is observed in the mixture both before and after reaction, indicative of catalyst stability. However, it is apparent that the surface of the originally spherical particles becomes rough after reaction and new large particles are formed as shown in Fig. 7(b). Combined with the average crystallite size of Zn determined by XRD (Table 4) and ICP-OES results (Tables 6(a), 6(b)), it can be hypothesised that these morphological changes to zinc powder are because Zn participates in the reaction and remains in the liquid product as Zn^{2+}. From the XRD pattern (Fig. 5), $ZnCO_3$ is known to be formed after the reaction. This agglomerates with K_2CO_3-NaBr-ZnO catalyst particles (Fig. 7(d)). The new $ZnCO_3$ particles with an average crystalline size of 42 nm are obtained through the reaction of $Zn(OH)_2$ (the hydrolysis product of $Zn(OCH_3)_2$) with CO_2 (Fujita et al., 1992). This process is accompanied by the formation of methanol, which promotes the transesterification reaction to generate DMC (Scheme 5, Route 2).

EDX spectroscopy was employed in order to obtain information on the elemental composition of the solid catalyst and the distribution of elements on catalyst surface and to investigate the effect of calcination. Table 5 shows that the zinc content decreases by 18 mass% as a consequence of the participation of zinc (powder) in the reaction. The Na^+ and O^{2-} content should in principle increase in percentage terms as a result, however only the O^{2-} content increases. This is ascribed to the formation of $ZnCO_3$. The decrease of Na^+ is due to the leaching of Na^+ from the catalyst surface into the reaction solution. The elemental composition of solid catalyst by EDX analysis is consistent with ICP-OES analysis results (Table 6 (a)).

EDX-mapping also indicates that the distribution of elements on the catalyst surface is essentially unchanged before and after calcination (Table 5) as the structure of catalyst remains stable below 720 °C. Moreover, Fig. 8 shows that the active materials are uniformly dispersed on the surface of the support after calcination and that this process therefore does not have a negative impact on catalyst performance.

3.3.4. ICP-OES and AAS analysis

ICP-OES and AAS analysis of both solid and liquid samples was carried out in order to determine the quantity of Zn, Na and K in solid catalyst and liquid product before and after reaction and therefore to identify any leaching of potentially catalytic material and hence potential homogenous catalytic contribution to the reaction. The results of ICP and AAS analysis of catalysts and liquid product solution are shown in Tables 6(a) and 6(b), respectively. Both of these indicate that there is little change in the total Zn^{2+} content in the K_2CO_3-NaBr-ZnO after reaction. It can therefore be assumed that ZnO content in the mixture of Zn powder and K_2CO_3-NaBr-ZnO also remains stable. However, when Zn powder is also present in the reaction mixture the mass of Zn powder is observed to decrease by ~ 30%. This indicates that Zn powder is directly involved in the reaction and is correlated with an increase in DMC selectivity (Table 6a, entry 3, 4). This is consistent with the results of SEM-EDX analysis, where zinc mass was seen to decrease by 18% post-reaction (Table 5). Moreover, XRD results (Table 4) also indicate that the average crystallite size of zinc powder decreases from 54 nm to 45 nm after reaction. It is therefore hypothesised that a fraction of Zn powder participates in the reaction, converting to solubilised Zn^{2+}.

While Zn powder (if added) shows a significant reduction in mass during reaction, ICP-OES and AAS data indicate that the ZnO support is in contrast highly stable during the reaction. Alkali metal ions, K^+ and Na^+, however leach into solution and potentially react with the feedstock (Table 6b). In the absence of Zn powder, K_2CO_3-NaBr-ZnO exhibits a loss of 99.8 wt% K^+ post reaction, while Na^+ diminishes by 98.2 wt% (Table 6(a)). With the addition of Zn powder, the stability of the catalyst increases as evidenced by the increased retention of alkali metals in the solid catalyst (Table 6 (a)). Potassium content decreases 76.5 wt% and Na^+ by only 16 wt %. Two hypotheses are proposed to explain this phenomenon.

Table 4
Average crystalline size of particles before and after reaction. '-' indicates that a crystalline phase is not observed in the diffractogram. '*' indicates that the corresponding peak is present but is beneath the size limit to accurately determine the crystallite size.

	Average crystalline size (nm)		
	ZnO	Zn	$ZnCO_3$
Catalyst	46 ± 6	–	–
Catalyst (after reaction)	43 ± 5	–	*
Mixture of catalyst and Zn	44 ± 4	54 ± 4	–
Mixture of catalyst and Zn (after reaction)	50 ± 3	45 ± 2	42 ± 4

Table 5
Elemental composition of the catalyst and the mixture of catalyst and zinc powder by EDX spectroscopy.

Mass (%)	Catalyst		Mixture of catalyst and Zn	
	Before calcination	After calcination	Before reaction	After reaction
Na	8.78	10.89	8.94	6.89
Zn	60.22	55.57	60.55	42.42
O	31.01	33.54	30.50	50.68
Mg	–	–	–	–

For each sample, a minimum of 5 different measurements were conducted and the experimental error is within ± 3%.

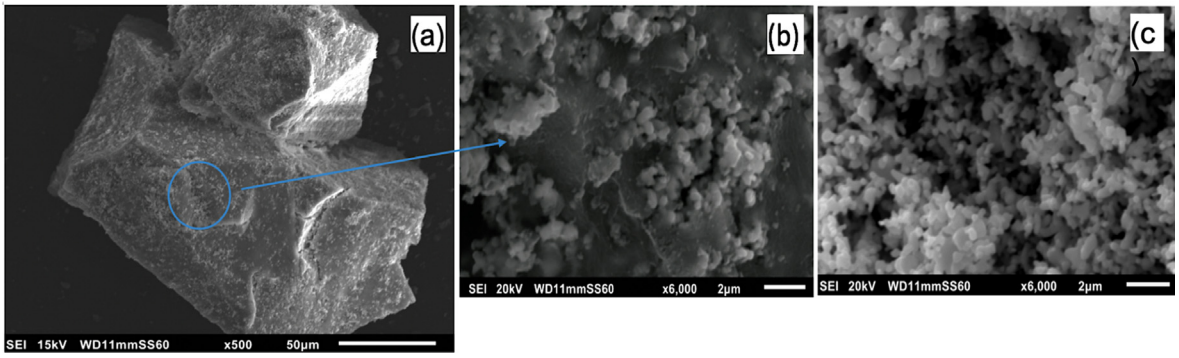

Fig. 6. SEM images of the solids resulting from reactions involving $Mg(OCH_3)_2$: (a) reaction with K_2CO_3-NaBr-ZnO catalyst, CO_2, propylene oxide, methanol and $Mg(OCH_3)_2$; (b) Higher magnification (6000x) image of identified region in (a); and (c) K_2CO_3-NaBr-ZnO catalyst prior to reaction (6000x).

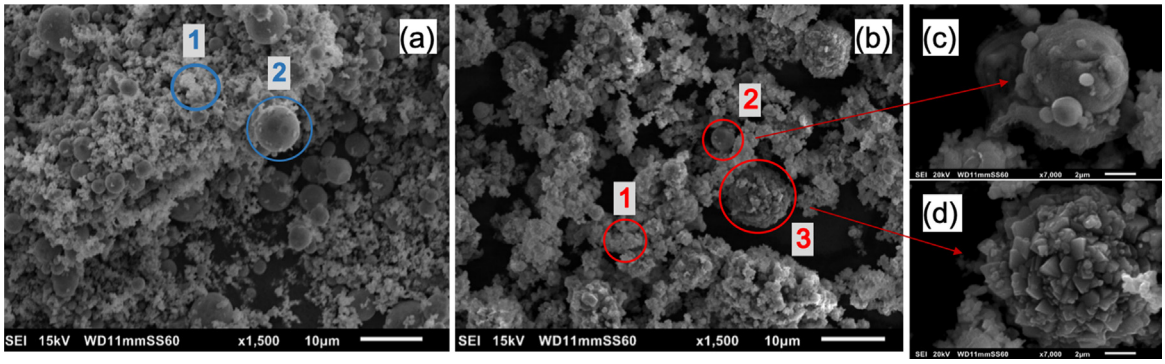

Fig. 7. Surface morphology of the catalyst and mixtures of catalyst and Zn powder. (a) mixture of fresh catalyst and Zn (b) mixture of spent catalyst and Zn (c) spent zinc particles with a higher magnification (7000x) (d) new formed particle with a higher magnification (7000x).

Table 6a
Composition of fresh and used catalysts, (12% K_2CO_3 – 17.5% NaBr-ZnO) as determined by AAS and ICP-OES.

Entry	Sample	AAS analysis (mg/g_{sample})			ICP-OES analysis (mg/g_{sample})		
		Total Zn^{2+}	Zn mass	ZnO mass	Total Zn^{2+}	K mass	Na mass
1	Fresh catalyst	786.5	0	984.7	731.0	4.390	2.900
2	Post-reaction catalyst	793.0	0	992.8	741.0	0.008	0.052
3	Fresh catalyst and Zn mixture	905.7	608.2	372.2	842.0	2.010	1.280
4	Post-reaction catalyst and Zn mixture	725.7	428.3	372.2	675.0	0.473	1.070

Table 6b
ICP-OES analysis of Zn, K and Na in the liquid products after reaction. Catalyst refers to 12% K_2CO_3 – 17.5% NaBr-ZnO.

Entry	Sample	Total Zn (mg/L)	K mass (mg/L)	Na mass (mg/L)
1	Catalyst	11.9	238.0	152.0
2	Mixture of catalyst and Zn powder	1950	197.0	13.0

Firstly, SEM images show that new large particles are formed due to the agglomeration of the catalyst and $ZnCO_3$ (Fig. 7 (d). This may hinder the interaction between surface Na^+ and K^+ and the reaction solution, thereby hindering dissolution. A second hypothesis is that Zn^{2+} content in solution increases during the reaction, thereby reducing the demand for K^+ and Na^+ in the DMC formation

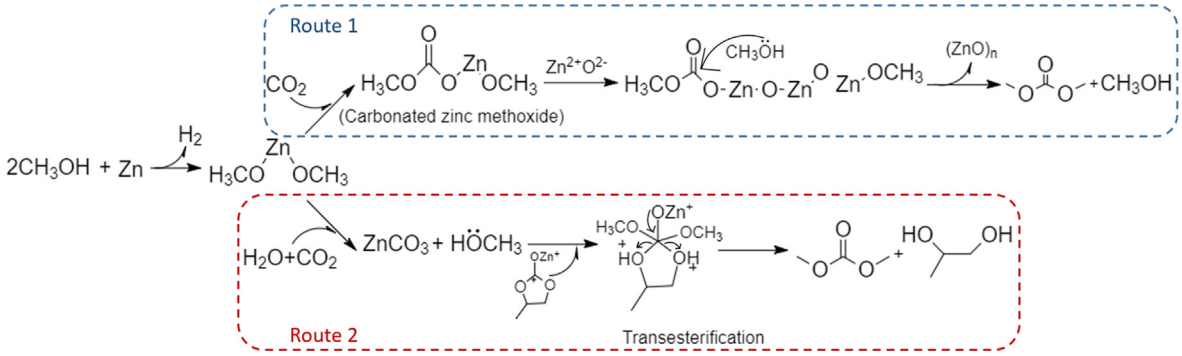

Scheme 5. Proposed new mechanism for DMC synthesis with the addition of Zn powder.

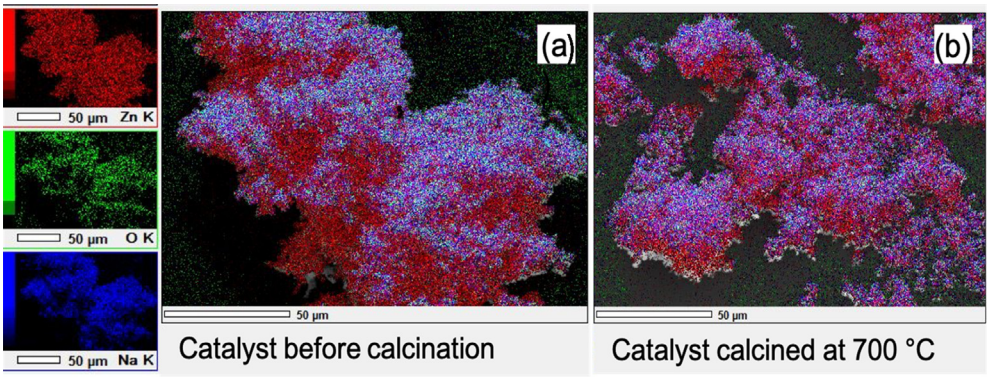

Fig. 8. The distribution of zinc (red), oxygen (green) and sodium (blue) on catalyst surface before and after calcination by EDX mapping: (a) catalyst before calcination; and (b) catalyst calcined at 700 °C. (For interpretation of the references to colour in this figure legend, the reader is referred to the web version of this article.)

reaction. According to hard and soft acids and bases (HSAB) theory, first proposed by Pearson, Lewis acids can be classified according to the stability of the metal complexes into: (i) hard Lewis acids (Na^+ and K^+); (ii) borderline Lewis acids (Zn^{2+}); and (iii) soft Lewis acids (Parr and Pearson, 1983). Generally, hard acids preferentially bind to hard bases to give ionic complexes, whereas soft acids bind to soft bases to yield covalent complexes. The oxygen atom of the carbonyl group in propylene carbonate displays the properties of a hard Lewis base (Laurence and Gal, 2009). The reactive polar covalent complex may therefore form when the oxygen of the C=O group attacks the Zn^{2+} ion in the transesterification reaction, contributing to the formation of DMC. Therefore, Zn^{2+} ions are more reactive to C=O of propylene carbonate than Na^+ and K^+ ions.

3.4. Proposed reaction mechanism

Zn powder was originally proposed as a dehydrating agent in DMC synthesis in order to reduce the production of propylene glycol from propylene oxide hydrolysis, thereby facilitating transesterification to the final product. However, herein (Section 3.2) it was shown that selectivity to PG does not decrease with the addition of Zn powder, however selectivity to DMC approximately doubles from 19.8% to 40.2%. Characterisation (Section 3.3) reveals that Zn powder may participate in the reaction, forming zinc methoxide ($Zn(OCH_3)_2$). This species may act as a homogeneous catalyst for the conversion of PC to DMC *via* transesterification. Dimethyl carbonate in the presence of zinc may therefore be generated through two proposed reactions (Scheme 5). Firstly, reaction of Zn with CO_2 and methanol to form carbonated zinc methoxide (CZM). The carbonate group of CZM then reacts with the unsaturated $Zn^{2+}O^{2-}$ Lewis acid-base pair on the catalyst surface and the intermediate bidentate carbonate is formed, the formation of which is supported by the presence of $Mg_{0.1}Zn_{0.9}O$ in XRD analysis (section 3.3.2, Fig. 4). The exchange of oxygen atoms in the bidentate carbonate with the oxygen atoms on the catalyst surface results in the migration of carbonate species on the catalyst surface, thereby facilitating the formation of DMC, with the release of ZnO polymeride. The second proposed reaction pathway involves the formation of additional methoxy groups, which can attack the carbon atom of C=O in the transesterification reaction. As observed by XRD data (Table 4) and SEM images (Fig. 7) of the spent catalyst and zinc powder, $ZnCO_3$ with an average particle size of 42 nm is formed during reaction. This is accompanied by the release of $-CH_3O$ as a consequence of the reaction of zinc methoxide with CO_2 and H_2O. Combining these two reaction pathways, an overall mechanism is presented in Scheme 5.

It is proposed that at higher pressures of carbon dioxide than those studied herein, $Zn(OCH_3)_2$ may directly catalyse carbon–carbon bond formation between methanol and CO_2, allowing the direct synthesis of DMC under mild conditions without PO. This represents a promising avenue for further study.

However, the proposed mechanism is only based on the experimental observation and detailed analysis is needed to support the proposed mechanism. For instance, in order to identify if zinc methoxide is a necessary reaction intermediate, ^{13}C labelled zinc methoxide and/or ^{13}C labelled magnesium methoxide can be employed in the experiment to evaluate the proposed reaction pathways.

4. Conclusions

K_2CO_3-NaBr-ZnO has been employed as a catalyst in the synthesis of dimethyl carbonate from methanol, propylene oxide and

carbon dioxide. The addition of Zn powder to this system increases selectivity to DMC. Zn both promotes DMC formation through new reaction routes and increases the stability of the catalyst. Crucial intermediate products, zinc methoxide and carbonate zinc methoxide, are formed during reaction and promote the migration of carbonate species on the catalyst surface yielding increased quantities of DMC. Zinc powder has little effect on the cycloaddition reaction but has a dramatic influence on the transesterification reaction resulting in increased DMC production through the formation of methoxide species. Furthermore, high pressure is not a prerequisite for the transesterification reaction. CO_2 was found to inhibit the reverse cycloaddition reaction to form PO. Future investigations into the effects of different active species on the reaction steps in DMC synthesis are recommended.

Funding

EPSRC is acknowledged for support via grant EP/R026815/1 and, for SEM data, via EP/K001329/1, for SEM data.

CRediT authorship contribution statement

Ming Liu: Conceptualization, Methodology, Validation, Investigation, Resources, Writing - original draft, Writing - review & editing, Visualization, Funding acquisition. **Mariia Konstantinova:** Investigation, Writing - original draft, Writing - review & editing. **Leila Negahdar:** Methodology, Investigation, Writing - original draft, Writing - review & editing, Visualization, Supervision, Funding acquisition. **James McGregor:** Conceptualization, Methodology, Resources, Data curation, Writing - review & editing, Supervision, Project administration, Funding acquisition.

Declaration of Competing Interest

The authors declare that they have no known competing financial interests or personal relationships that could have appeared to influence the work reported in this paper.

Acknowledgements

EPSRC is acknowledged for support via grant EP/R026815/1 and, for SEM data, *via* EP/K001329/1, for SEM data. The authors also with to thank Dr. Benjamin M. Partridge, University of Sheffield, Department of Chemistry for discussions and advice on the proposed mechanisms.

Appendix A. Supplementary material

Supplementary data to this article can be found online at https://doi.org/10.1016/j.ces.2020.116267.

References

Aricò, F., Tundo, P., 2010. Dimethyl carbonate as a modern green reagent and solvent. Russ. Chem. Rev. https://doi.org/10.1070/rc2010v079n06abeh004113.

Balat, M., 2007. Production of biodiesel from vegetable oils: A survey. Energy Sources Part A Recover. Util. Environ. Eff. 29, 895–913. https://doi.org/10.1080/00908310500283359.

Bhanage, B.M., Fujita, S., Ikushima, Y., Arai, M., 2001. Synthesis of dimethyl carbonate and glycols from carbon dioxide , epoxides , and methanol using heterogeneous basic metal oxide catalysts with high activity and selectivity 219, 259–266.

Chang, Y., Jiang, T., Han, B., Liu, Z., Wu, W., Gao, L., Li, J., Gao, H., Zhao, G., Huang, J., 2004. One-pot synthesis of dimethyl carbonate and glycols from supercritical CO2, ethylene oxide or propylene oxide, and methanol. Appl. Catal. A Gen. 263, 179–186. https://doi.org/10.1016/j.apcata.2003.12.012.

Chen, E.Y.X., Marks, T.J., 2000. Cocatalysts for metal-catalyzed olefin polymerization: Activators, activation processes, and structure-activity relationships. Chem. Rev. 100, 1391–1434. https://doi.org/10.1021/cr980462j.

De, C., Lu, B., Lv, H., Yu, Y., Bai, Y., Cai, Q., 2009. One-pot synthesis of dimethyl carbonate from methanol, propylene oxide and carbon dioxide over supported choline hydroxide/MgO. Catal. Lett. 128, 459–464. https://doi.org/10.1007/s10562-008-9773-1.

Dimethyl Carbonate Market by Application (Polycarbonate, Solvent, Pharmaceutical, Pesticide) - Growth, Share, Opportnities & Competitive Analysis, 2017 - 2025, 2017.

Eta, V., Leino, A., 2010. Synthesis of Dimethyl Carbonate from Methanol and Carbon Dioxide: Circumventing Thermodynamic Limitations 9609–9617.

Eta, V., Mäki-Arvela, P., Leino, A.R., Kordás, K., Salmi, T., Murzin, D.Y., Mikkola, J.P., 2010. Synthesis of dimethyl carbonate from methanol and carbon dioxide: Circumventing thermodynamic limitations. Ind. Eng. Chem. Res. https://doi.org/10.1021/ie1012147.

Fierro, J.L.G., Melián-Cabrera, I., López Granados, M., 2002. Reverse topotactic transformation of a Cu-Zn-Al catalyst during wet Pd impregnation: Relevance for the performance in methanol synthesis from CO2/H2 mixtures. J. Catal. 210, 273–284. https://doi.org/10.1006/jcat.2002.3676.

Fujita, S. ichiro, Usui, M., Ohara, E., Takezawa, N., 1992. Methanol synthesis from carbon dioxide at atmospheric pressure over Cu/ZnO catalyst. Role of methoxide species formed on ZnO support. Catal. Letters 13, 349–358. https://doi.org/10.1007/BF00765037.

Jiang, Q., Yang, Y., 2004. The double component catalyst for the direct synthesis of dimethyl carbonate from carbon dioxide, propylene oxide and methanol. Catal. Lett. 95, 127–133. https://doi.org/10.1023/B:CATL.0000027285.38036.12.

Lagarde, F., Srour, H., Berthet, N., Oueslati, N., Bousquet, B., Nunes, A., Martinez, A., Dufaud, V., 2019. Investigating the role of SBA-15 silica on the activity of quaternary ammonium halides in the coupling of epoxides and CO2. J. CO2 Util. 34, 34–39. https://doi.org/10.1016/j.jcou.2019.05.023.

Laurence, C., Gal, J.F., 2009. Lewis Basicity and Affinity Scales: Data and Measurement, Lewis Basicity and Affinity Scales: Data and Measurement. https://doi.org/10.1002/9780470681909.

Li, L., Shi, S., Song, L., Guo, L., Wang, Y., Ma, H., Hou, J., Wang, H., 2015. One-step synthesis of dimethyl carbonate from carbon dioxide, propylene oxide and methanol over alkali halides promoted by crown ethers. J. Organomet. Chem. 794, 231–236. https://doi.org/10.1016/j.jorganchem.2015.07.010.

Li, Y., Zhao, X.Q., Wang, Y.J., 2005. Synthesis of dimethyl carbonate from methanol, propylene oxide and carbon dioxide over KOH/4A molecular sieve catalyst. Appl. Catal. A Gen. 279, 205–208. https://doi.org/10.1016/j.apcata.2004.10.030.

Liu, C., Zhang, S., Cai, B., Jin, Z., 2015. Low pressure one-pot synthesis of dimethyl carbonate catalyzed by an alkali carbonate. Cuihua Xuebao/Chinese J. Catal. 36, 1136–1141. https://doi.org/10.1016/S1872-2067(14)60309-0.

Liu, M., Liu, B., Liang, L., Wang, F., Shi, L., Sun, J., 2016. Design of bifunctional NH3I-Zn/SBA-15 single-component heterogeneous catalyst for chemical fixation of carbon dioxide to cyclic carbonates. J. Mol. Catal. A Chem. 418–419, 78–85. https://doi.org/10.1016/j.molcata.2016.03.037.

Martínez-Ferraté, O., Chacón, G., Bernardi, F., Grehl, T., Brüner, P., Dupont, J., 2018. Cycloaddition of carbon dioxide to epoxides catalysed by supported ionic liquids. Catal. Sci. Technol. 8, 3081–3089. https://doi.org/10.1039/c8cy00749g.

Murugan, C., Bajaj, H.C., 2010. Transesterification of propylene carbonate with methanol using Mg-Al-CO3 hydrotalcite as solid base catalyst. Indian J. Chem. - Sect. A Inorganic Phys. Theor. Anal. Chem. 49, 1182–1188.

Pacheco, M.A., Marshall, C.L., 1997. Review of dimethyl carbonate (DMC) manufacture and its characteristics as a fuel additive. Energy and Fuels. https://doi.org/10.1021/ef9600974.

Parr, R.G., Pearson, R.G., 1983. Absolute Hardness: Companion Parameter to Absolute Electronegativity. J. Am. Chem. Soc. 105, 7512–7516. https://doi.org/10.1021/ja00364a005.

Patterson, A.L., 1939. The scherrer formula for X-ray particle size determination. Phys. Rev. 56, 978–982. https://doi.org/10.1103/PhysRev.56.978.

Sakakura, T., Kohno, K., 2009. The synthesis of organic carbonates from carbon dioxide. Chem. Commun. https://doi.org/10.1039/b819997c.

Selva, M., Marques, C.A., Tundo, P., 1994. Selective mono-methylation of arylacetonitriles and methyl arylacetates by dimethyl carbonate. J. Chem. Soc. Perkin Trans. 1.

Simo, M., Sivashanmugam, S., Brown, C.J., Hlavacek, V., 2009. Adsorption/desorption of water and ethanol on 3A zeolite in near-adiabatic fixed bed. Ind. Eng. Chem. Res. 48, 9247–9260. https://doi.org/10.1021/ie900446v.

Subramanian, S., Park, J., Byun, J., Jung, Y., Yavuz, C.T., 2018. Highly Efficient Catalytic Cyclic Carbonate Formation by Pyridyl Salicylimines. ACS Appl. Mater. Interfaces 10, 9478–9484. https://doi.org/10.1021/acsami.8b00485.

Suleman, S., Younus, H.A., Ahmad, N., Khattak, Z.A.K., Ullah, H., Chaemchuen, S., Verpoort, F., 2019. CO2 insertion into epoxides using cesium salts as catalysts at ambient pressure. Catal. Sci. Technol. 9, 3868–3873. https://doi.org/10.1039/c9cy00694j.

Sun, C., Qiu, F., Yang, D., Ye, B., 2014. Preparation of biodiesel from soybean oil catalyzed by Al-Ca hydrotalcite loaded with K2CO3 as heterogeneous solid base catalyst. Fuel Process. Technol. 126, 383–391. https://doi.org/10.1016/j.fuproc.2014.05.021.

The Royal Society, 2017. The potential and limitations of using carbon dioxide [WWW Document].

Tian, J.S., Miao, C.X., Wang, J.Q., Cai, F., Du, Y., Zhao, Y., He, L.N., 2007. Efficient synthesis of dimethyl carbonate from methanol, propylene oxide and CO2 catalyzed by recyclable inorganic base/phosphonium halide-functionalized

polyethylene glycol. Green Chem. 9, 566–657. https://doi.org/10.1039/b614259a.

Truong, C.C., Mishra, D.K., 2020. Recent advances in the catalytic fixation of carbon dioxide to value-added chemicals over alkali metal salts. J. CO2 Util. 41,. https://doi.org/10.1016/j.jcou.2020.101252 101252.

Wang, J.Q., Dong, K., Cheng, W.G., Sun, J., Zhang, S.J., 2012. Insights into quaternary ammonium salts-catalyzed fixation carbon dioxide with epoxides. Catal. Sci. Technol. 2, 1480–1484. https://doi.org/10.1039/c2cy20103h.

Wang, Y., Jia, D., Zhu, Z., Sun, Y., 2016. Synthesis of diethyl carbonate from carbon dioxide, propylene oxide and ethanol over KNO3-CeO2 and KBr-KNO3-CeO2 catalysts. Catalysts 6, 52. https://doi.org/10.3390/catal6040052.

Xu, W., Ji, S., Quan, W., Yu, J., 2013. One-Pot Synthesis of Dimethyl Carbonate over Basic Zeolite Catalysts. Mod. Res. Catal. 02, 22–27. https://doi.org/10.4236/mrc.2013.22A004.